EXOSKELETONS

Bilateral Back Extensor Exosuit for multidimensional assistance and prevention of spinal injuries

Jae In Kim[1,2]†, Jaeyoun Choi[2]†, Junhyung Kim[2,3,4]†, Junkyung Song[5,6], Jaebum Park[5,6], Yong-Lae Park[2,3,4]*

Lumbar spine injuries resulting from heavy or repetitive lifting remain a prevalent concern in workplaces. Back-support devices have been developed to mitigate these injuries by aiding workers during lifting tasks. However, existing devices often fall short in providing multidimensional force assistance for asymmetric lifting, an essential feature for practical workplace use. In addition, validation of device safety across the entire human spine has been lacking. This paper introduces the Bilateral Back Extensor Exosuit (BBEX), a robotic back-support device designed to address both functionality and safety concerns. The design of the BBEX draws inspiration from the anatomical characteristics of the human spine and back extensor muscles. Using a multi–degree-of-freedom architecture and serially connected linear actuators, the device's components are strategically arranged to closely mimic the biomechanics of the human spine and back extensor muscles. To establish the efficacy and safety of the BBEX, a series of experiments with human participants was conducted. Eleven healthy male participants engaged in symmetric and asymmetric lifting tasks while wearing the BBEX. The results confirm the ability of the BBEX to provide effective multidimensional force assistance. Moreover, comprehensive safety validation was achieved through analyses of muscle fatigue in the upper and the lower erector spinae muscles, as well as mechanical loading on spinal joints during both lifting scenarios. By seamlessly integrating functionality inspired by human biomechanics with a focus on safety, this study offers a promising solution to address the persistent challenge of preventing lumbar spine injuries in demanding work environments.

INTRODUCTION

Heavy or repetitive lifting-induced lower back injuries are the most prevalent workplace afflictions and impose substantial physical and economic strains on individuals, communities, and industries (*1*–*4*). The act of lifting heavy objects subjects the spine to substantial mechanical loads, potentially leading to force-triggered conditions, such as intervertebral disc herniation, prolapse, or protrusion (*5*–*10*). Simultaneously, repetitive lifting, even with lighter objects, leads to fatigue in the back extensor muscles, resulting in diminished strength and potential muscle or tendon strains (*11*–*13*). These cumulative injuries often contribute to the development of low back pain (LBP), with excessive mechanical loading and muscle fatigue standing out as prominent risk factors associated with lifting-related LBP (*14*–*16*).

Amid their growing popularity for alleviating risk factors and relieving lower back strain, wearable back-support devices have encountered substantial challenges, particularly in facilitating multidimensional movement during asymmetric lifting, a crucial functionality for their practical application. Notably, although established devices like Bendezy, WMRD, BNDR, Waist Power-Assist, Passive Spine Exoskeleton, RoboMate, SIAT waist EXO, and BackX (S-model) have demonstrated their effectiveness in assisting unidirectional lifting (specifically flexion/extension in the sagittal plane) (*17*–*26*), they are limited in providing comprehensive multidimensional support because they do not facilitate the natural movements of the torso in multiple directions in their designs. In industrial contexts, frequent multidimensional lifting demands render such devices less efficient, hampering overall work performance. Alternatives allowing multidimensional lower back movements, such as Laevo, Hyundai H-WEX, Soft Power Suit, BackX (Model AC), ATOUN, AWN-03 Panasonic, and Hip Joint Exoskeleton, provide solely unidirectional force assistance (*27*–*32*). Owing to a lack of additional degrees of freedom (DoFs), these devices are ineffective in adequately supporting the lower back during multidimensional asymmetric lifting scenarios.

Moreover, prior investigations have inadequately addressed the comprehensive safety validation of back-support devices across the entirety of the human spine. The conventional safety assessment for such devices has conventionally centered around the reduction of joint reaction forces exclusively at the lumbosacral joint (*33*–*35*). However, the potential risk of amplified joint reaction forces on other spinal segments stemming from the use of assistive devices has often been overlooked. For instance, assistive devices using hip joint–generated moments to facilitate back extension may inadvertently elevate shear forces on the mid-to-upper lumbar joints, given the perpendicular application of assistive forces relative to the spine. Similarly, assistive devices designed to deliver tensional forces parallel to the back might exacerbate compression forces if improperly aligned with the spine, particularly during asymmetric lifting maneuvers. Despite the emergence of multidimensional support devices like the Lower-Back Robotic Exoskeleton, SPEXOR, VT-Lowe's, Paexo Back, Spine-Inspired Continuum Soft Exoskeleton, and ABX (*36*–*43*), uncertainty persists regarding the comprehensive spinal safety ensured by these devices, owing to the scarcity of biomechanical outcome data in the limited scope of evaluations.

This study introduces the Bilateral Back Extensor Exosuit (BBEX), a back-support wearable robotic device aimed at achieving multidimensional force assistance and comprehensive spinal safety. Drawing

[1]Samsung Electronics, Suwon, Korea. [2]Department of Mechanical Engineering, Seoul National University, Seoul 08826, Korea. [3]Institute of Advanced Machines and Design, Seoul National University, Seoul 08826, Korea. [4]Institute of Engineering Research, Seoul National University, Seoul 08826, Korea. [5]Department of Physical Education, Seoul National University, Seoul 08826, Korea. [6]Institute of Sport Science, Seoul National University, Seoul 08826, Korea.
*Corresponding author. Email: ylpark@snu.ac.kr
†These authors contributed equally to this work.

inspiration from the anatomical characteristics of the human spine and back extensor muscles, the BBEX comprises multi-DoF structures and serially connected linear actuators specifically arranged to align with the functional attributes of the human spine and the back extensor muscles, respectively (Fig. 1). By harnessing its sufficient DoFs, the BBEX enables natural spinal movement across various ranges, whereas its assistive forces, in alignment with the back muscles, deliver multidimensional support similar to the actions of these muscles. This synchronization of forces in the BBEX enables effective assistance to the back extensor muscles, effectively reducing fatigue in the back muscles and alleviating compression forces on the spinal joints.

RESULTS

Bilateral Back Extensor Exosuit

The Bilateral Back Extensor Exosuit (BBEX) was named after the observed morphological and functional similarities between the device and the human spine, particularly with respect to the back extensor muscles. For an overview of the BBEX, please refer to movie S1. The BBEX primarily consisted of vertebra modules, twisted elastic rotary-rail actuators (TERRAs), back interface parts, and electric components incorporating brushless dc electric motors and force/torque sensors (Fig. 2). The weight distribution of the BBEX included a 0.42-kg battery, a 0.46-kg anchoring suit, and a combined weight of 4.87 kg for the actuator and the computing board, resulting in the total weight of the BBEX of 5.75 kg (Supplementary Methods and fig. S1). The mechanical implementations of the BBEX are described in the following subsections.

Design concept

The human spine exhibits a kinematic arrangement characterized by a series of interconnected rigid structures, enabling complex multi-DoF movements. Comprising numerous vertebrae and intervertebral joints sequentially linked, the human spine represents an intricate biomechanical design where each intervertebral joint encompasses an interbody joint housing an intervertebral disc, accompanied by a pair of facet joints. In particular, the compliant and adaptable composition of the intervertebral disc primarily supports vertebral compression, whereas the facet joints contribute to the kinematic attributes governing bending and twisting motions of the vertebrae (*44*–*46*). These dynamic features, provided by the interplay between the disc and the facet joints, grant each vertebra three rotational DoFs: flexion-extension, lateral bending, and axial rotation. The sequential fusion of these vertebrae enables the multi-DoF movements of the human spine.

The multi-DoF movements of the human spine are orchestrated by the back extensor muscles surrounding the spine, among which the erector spinae muscles play a critical role in this complex interplay. These muscles have a bilateral configuration in relation to the spine, seamlessly integrating with the spinal anatomy within a range of back movements. This bilateral alignment facilitates the erector spinae muscles to assist the motions of the spine across various DoFs, such as extension through bilateral muscle contraction, lateral bending through unilateral contraction of a single muscle, and axial rotation through contraction in a twisted configuration. The multi-DoF movements of the spine enable humans to perform various lifting tasks. In particular, asymmetric lifting requires a combination of spinal flexion-extension, lateral bending, and axial rotation. To effectively assist such lifting movements, multidimensional support is essential. When properly applied to the upper body, multidimensional assistance outperforms unidimensional assistance substantially, resulting in reductions in muscle forces and joint reaction forces on arbitrary spinal joints (a comparison between multidimensional assistance and unidimensional assistance can be found in the Supplementary Discussion and fig. S2).

Leveraging the anatomical characteristics of the human spine and the erector spinae muscles, we devised a multidimensional assistance mechanism, the secondary erector spinae (SES) mechanism. The SES mechanism is enabled by multiple actuation modules connected in series, each of which consists of a vertebra block, ball-and-socket joints, and linear actuators, showing a bilateral configuration analogous to that of the erector spinae muscles (Fig. 1A). The combination of the ball-and-socket joints and the linear actuators allows each vertebra block to rotate in three DoFs, closely resembling the mobility of the human vertebra (Fig. 1B, i to iii). Consequently, the SES mechanism aligns with the spine and readily adapts to the spine's various movements. Moreover, this kinematic alignment ensures that the linear actuators of the SES mechanism kinetically align with the erector spinae muscles, providing multidirectional force assistance similar to those muscles. These assistive forces, aligned with the erector spinae muscles, have the potential to effectively reduce muscle activation and spinal loading across all spinal joints. We showed that kinetically aligned assistive forces can alleviate both the back muscle forces and joint compression forces on various spinal joints. Moreover, in the cases where back muscle forces mainly contribute to joint shear forces, the assistive forces can effectively reduce them. This is due to the external assistive forces generating increased momentum with the same applied force, a result of a longer moment

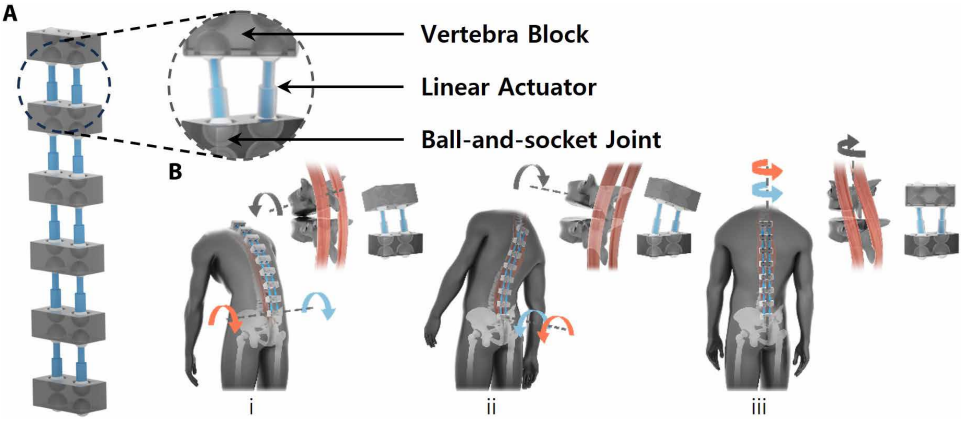

Fig. 1. SES mechanism. (**A**) Configuration of the SES mechanism. (**B**) The SES mechanism has multi-DoFs as the spine, and its bilateral actuators can assist (i) flexion-extension, (ii) lateral bending, and (iii) axial rotation motions similar to back extensor muscles. The red arrows represent the moments generated by back extensor muscles, the blue arrows represent the moments generated by the SES mechanism, and the gray arrows represent the rotations of the vertebrae.

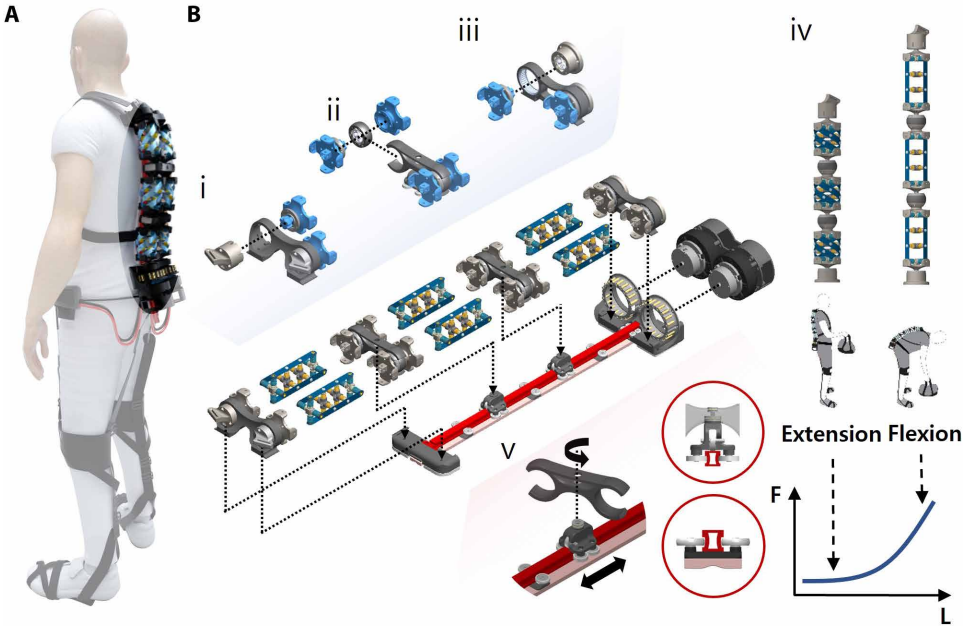

Fig. 2. Overview and exploded-view of the BBEX. (**A**) Overview. (**B**) Exploded view. The blue-colored parts independently work as a ball-and-socket joint at the (i) upper, (ii) middle, and (iii) lower modules. (iv) The 4R-TERRA that creates linear motion by twisting in a helical shape works as a linear actuator. The 4R-TERRA generates a larger force as its length increases so that the BBEX can efficiently provide a considerable assistive force for flexion posture. (v) Middle modules have two additional DoFs through the moving blocks.

arm, thereby effectively diminishing muscle forces and their subsequent reaction forces (benefit of assistive forces aligned with back muscles can be found in the Supplementary Discussion and fig. S3).

Vertebra module

The vertebra module was designed to integrate both the vertebra block and ball-socket joint for the SES mechanism. To achieve optimal alignment of the BBEX with the host system (the human spine), it is necessary to have the same number of vertebra modules as vertebrae that comprise the spine. However, this requirement increases the complexity of the design. In an effort to streamline this complexity, we designed the BBEX with four vertebra modules: one for the upper region, two for the middle region, and one for the lower region of the spine (Fig. 2B, i to iii). Each module consists of one vertebra block and two constant-velocity (CV) joints, with each CV joint functioning as a ball-and-socket joint.

In the upper module, the housing for the CV joint was securely attached to the vertebra block, with the blue-flanged shaft serving as the ball-and-socket joint (Fig. 2Bi). In the middle module, an additional layer of functionality was introduced by linking the ball-shaped housing of the CV joint with the module's socket, allowing for the independent ball-and-socket motion for both the blue-flanged shaft and the ball-shaped housing (Fig. 2Bii). Moving to the lower module, the housing was inserted into a cylindrical bearing and connected to the motor, with the blue-flanged shaft again acting as a ball-and-socket joint (Fig. 2Biii). Detailed information on the vertebra module can be found in the Supplementary Methods and fig. S1.

Four-rail twisted elastic rotary-rail actuator

A four-rail twisted elastic rotary-rail actuator (4R-TERRA), an improvement on the original TERRA (*47*) featuring four rails, was developed to serve as the linear actuator of the SES mechanism. The 4R-TERRA was tailored to seamlessly integrate with the proposed wearable device, satisfying the required stroke length and durability. Functioning as a compliant linear actuator, the 4R-TERRA uses a helical twisting mechanism to produce linear motion (Fig. 2Biv).

Human skeletal muscles show length-dependent characteristics, generally exhibiting a decrease in active muscle force as the length of the muscle increases, with an increased reliance on passive tension (*48*). Therefore, externally supplementing the reduced active muscle forces in the back during a flexion posture for lifting, where muscles are elongated, is effective in preventing injuries associated with overuse of the back muscles and the muscle strain.

In contrast, the 4R-TERRA shows characteristics opposite to those of muscles, exerting greater force as it lengthens with the same input torque. This unique property suggests that the 4R-TERRA can play a complementary role to muscles, offering a distinct advantage in its application within our device. Also, given that greater assistive force is required in a flexion posture compared with an extension posture during lifting tasks, the 4R-TERRA can efficiently supply the necessary assistance with minimal input torques when elongated in a flexion posture (Supplementary Methods, fig. S4, and movie S2).

For the task at hand, a total of six 4R-TERRAs were used, with three units connected in series via CV joints to realize a bilateral configuration. The motor attached to the lowermost CV joint initiates rotation, and the serially connected 4R-TERRAs rotate uniformly while maintaining consistent length, because of the shared rotational function of the CV joint at both ends.

Back interface for spinal alignment

To ensure the alignment of the BBEX's centerline with the wearer's back, we devised a system using a combination of stretchable elastomer, guide bearings, and a flexible column. The stretchable elastomer was strategically positioned at the lower part of the BBEX, establishing direct contact with the wearer's back. Within this elastomer, four guide bearings were integrated and evenly distributed along its surface. Linked to these guide bearings is the flexible column, designed with an I-shaped cross section. As the wearer's back undergoes movement, the stretchable elastomer elongates while maintaining continuous contact with the back, consequently inducing a synchronized extension among the guide bearings. This, in turn, imparts a corresponding configuration to the flexible column, ensuring alignment with the centerline of the wearer's back.

Each vertebra module of the BBEX is coupled with the flexible column, ensuring that the centerline of the BBEX corresponds to that of the back. However, because of the uniform length of the serially connected 4R-TERRAs, additional DoFs are needed to facilitate the optimal functionality of the BBEX across a diverse range of back movements. In particular, each middle module requires two additional DoFs (Supplementary Discussion, fig. S5, and movie S3).

To address this requirement, we incorporated moving blocks into the system. These blocks introduce extra mobility to the middle modules, enabling them to both slide and rotate alongside the flexible column (Fig. 2Bv). Through this multi-DoF back interface, the BBEX successfully achieves and maintains spinal alignment during a wide range of back movements.

Textile-based anchoring mechanism

The design of our textile-based anchoring mechanism was inspired by the approach introduced by Asbeck *et al.* (*49*) and aimed to efficiently and comfortably transmit the assistive force generated by the BBEX to the wearer. For efficient force transmission, it is crucial for the anchoring mechanism to have a high suit-human series stiffness, which accounts not only for the stiffness of the device but also for the stiffness of the body parts to which the assistive force is applied. The high suit-human series stiffness reduces power loss caused by structural deformation of the device or the body, thus achieving a high efficiency in force transmission. To achieve this, we used high-stiffness materials like Bowden cables and straps and strategically selected body regions with minimal deformation, including the feet, shoulders, and back, to increase the suit-human series stiffness (Fig. 3A). For the wearer to be comfortable, the anchoring mechanism needs to be designed in a way that the assistive force is applied to the body in the form of a normal force. Applying an assistive motion via a shear force would require relatively high pressure on the wearer's skin to prevent device slippage, leading to discomfort. To align with these criteria, we designed both the lower and upper anchoring mechanisms (Fig. 3B).

The lower anchoring mechanism features a Bowden cable and its sheath, a high-stiffness strap, a knee band, and an overshoe. The Bowden cable sheath was affixed to the bottom module, encircling the hip joint, with the Bowden cable passing inside the sheath with minimal friction. Each end of the Bowden cable was connected to the knee band and the overshoe via the straps, creating a high-stiffness connection line from the bottom module to the overshoe. In addition, the foot, where the assistive force is transmitted, exhibits a relatively high stiffness among the lower extremities. Consequently, the bottom module of the BBEX remained firmly anchored with minimal deformation during the generation of assistive forces. The presence of the Bowden cable surrounding the hip joints allowed for unhindered hip motions (Fig. 3Cii). When the hip is flexed, the anterior cable becomes shorter, but the posterior cable is longer at the same time. These complementary movements allow for flexion and extension without constraining the natural movements of the hip joints (see movie S4).

The upper anchoring mechanism consists of straps for the shoulders, the sternum, and the back. The shoulder straps were attached to the top module of the BBEX and connected to the back strap through the sternum strap. This torso-enveloped line, formed by the high stiffness straps, was designed to pass over the area with a high body stiffness. Therefore, the top module of the BBEX was firmly anchored, and the assistive force was efficiently transmitted to the wearer. Also, the torso-enveloped line was designed to align the line of nonextension of the upper body, a length that remains consistent during various trunk motions (*50*). Thus, the upper anchoring mechanism does not restrict the range of trunk motion (Fig. 3Ci).

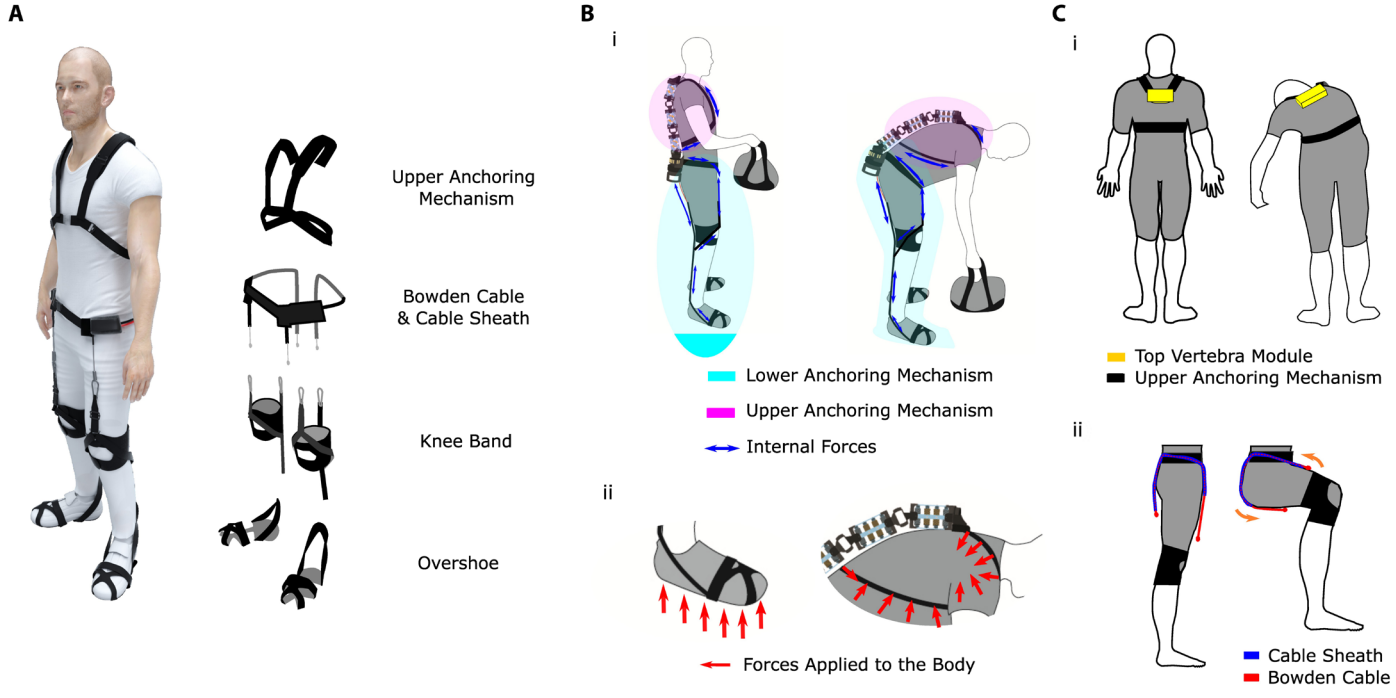

Fig. 3. Structure and principle of textile-based anchoring mechanism. (**A**) Configuration of the anchoring mechanism. (**B**) Forces in the anchoring mechanism. (i) Assistive force is transmitted to the body by high-stiffness material. (ii) Assistive force from the BBEX is transmitted to the feet, shoulders, chest, and back in a direction perpendicular to the skin surface. (**C**) Views of the (i) upper and (ii) lower anchoring mechanisms during various movements. The length of the upper anchoring mechanism does not change because it is placed on the lines of nonextension. The lower anchoring mechanism can allow hip flexion and extension motion because of the Bowden cable and cable sheath.

Validation with human participants

ROM and spinal alignment

Through an experiment for functional testing, we confirmed that the BBEX did not impede the wearer's range of motion (ROM), as shown in Fig. 4. When the BBEX was worn, the peak joint angles for lumbar flexion, lateral flexion, and axial rotation decreased by 2.49, 0.03, and 0.01%, respectively. However, the result of paired *t* tests verified that these reductions are statistically insignificant. Furthermore, we confirmed that the BBEX achieved a high alignment with the wearer's spine, with cosine similarities in all three directions measuring 0.98 each (Supplementary Methods, fig. S6, and movie S5).

Posture estimation and multi-DoF assistance

We confirmed that the BBEX estimated the wearer's posture with high accuracy in both symmetric and asymmetric lifting tasks. The wearer's posture was estimated through the kinematic model of the BBEX (Supplementary Methods and fig. S7). The total postural errors of the symmetric and asymmetric lifting tasks, averaged over all the participants with 30 lifts, are 21.99 ± 3.12 mm and 22.19 ± 3.60 mm, respectively. The mean postural errors during a single lifting, averaged for all participants, are shown in Fig. 5A (see movie S6 for visualization of the posture estimation). In both tasks, the postural errors were relatively large in the extension posture (0 and 8 s). The errors gradually decreased during the period of lowering the back and increased as the wearer approached the flexion posture (Supplementary Discussion and fig. S8).

We also confirmed that the BBEX provided multi-DoF assistance by modulating the assistive forces of the bilateral 4R-TERRAs. On the basis of the estimated wearer's posture, the BBEX actively controlled its assistance to compensate for the torque generated by the external load in both symmetric and asymmetric lifting tasks. The mean assistive forces and assistive torques, averaged for all participants, for each task during a single lift are shown in Fig. 5 (B and C). This result indicates that the BBEX provides multidimensional assistance on the basis of the wearer's posture (Supplementary Discussion and fig. S9).

HR and rating of perceived exertion

We evaluated the effect of the BBEX on physical intensity level: heart rate (HR) and rate of perceived exertion (RPE) (Fig. 6A). In both symmetric and asymmetric lifting tasks, the BBEX reduced the physical intensity level. A two-way repeated measures analysis of variance (ANOVA) revealed a significance of the main effect of the BBEX on both HR and RPE. Subsequent paired *t* tests further confirmed that the BBEX exerted a statistically significant effect on HR and RPE. The ANOVA and post hoc paired *t* test results are summarized in table S1. The HR with and without the BBEX increased by 15.40 and 23.14% during the symmetric lifting task, respectively, and by 13.15 and 26.53% during the asymmetric lifting task. This shows that the BBEX reduced the final HR by 18.90 and 28.40% in the symmetric and the asymmetric lifting tasks, respectively. Also, the RPE with and without the BBEX increased by 50.75 and 53.50%, respectively, during the symmetric lifting task and by 50.56 and 59.72%, respectively, during the asymmetric lifting task. This indicates that the BBEX reduced the final RPE by 7.89 and 10.70% in the symmetric and the asymmetric lifting tasks, respectively. These results indicated that the BBEX lowered exercise intensity in physiological effects (HR) and participants' perception levels (RPE).

Muscle fatigue

We analyzed the effect of the BBEX on muscle fatigue (Fig. 6B). In both symmetric and asymmetric lifting tasks, the BBEX reduced muscle fatigue of the lower erector spinae (LE) and upper erector spinae (UE). A two-way repeated measures ANOVA revealed a significance of the main effect of the BBEX on the median frequency (MDF) of both LE and UE. Subsequent paired *t* tests further confirmed that the BBEX exerted a statistically significant effect on the MDF of LE and UE. For the LE, the MDF with and without the BBEX decreased by 22.70 and 27.56%, respectively, during the symmetric lifting task and by 18.10 and 30.56%, respectively, during the asymmetric lifting task. This shows that the BBEX suppressed the final LE muscle fatigue (MDF reduction) by 17.69 and 40.78% in the symmetric and the asymmetric lifting tasks, respectively. For the UE, the MDF with and without the BBEX decreased by 17.98 and 22.65%, respectively, during the symmetric lifting task and by 10.81 and 22.94%, respectively, during the asymmetric lifting task. This indicates that the BBEX suppressed the final UE muscle fatigue (MDF reduction)

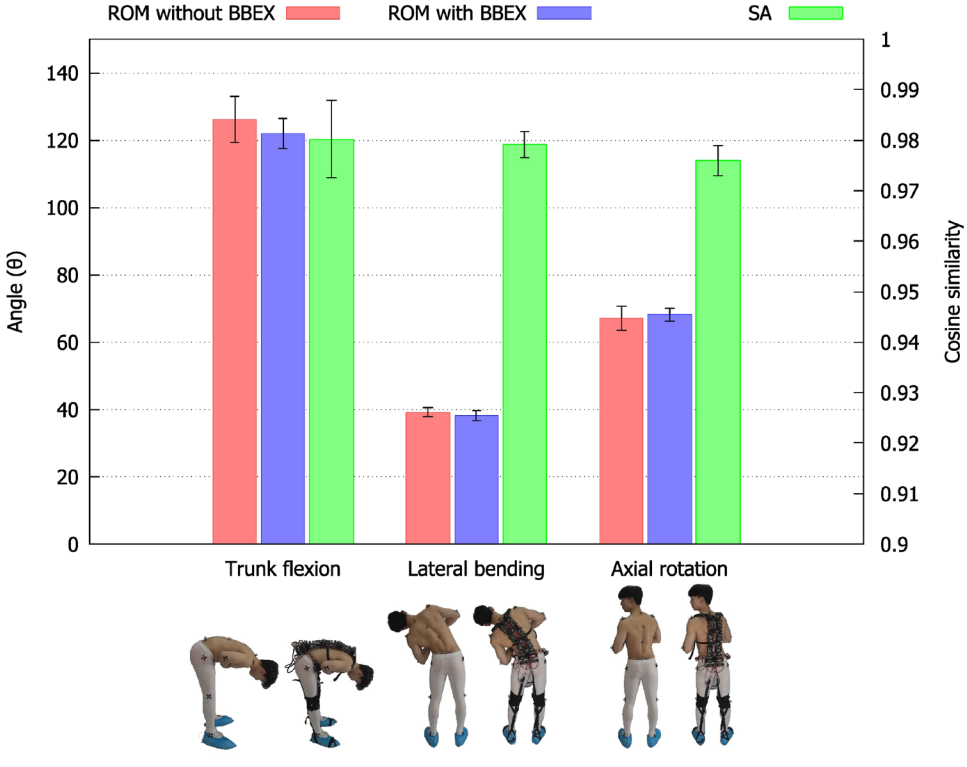

Fig. 4. ROM and spinal alignment. Peak joint angles of spinal flexion, lateral flexion, and axial rotation were calculated for the ROM using the inverse kinematics tool of the OpenSim. Cosine similarities were calculated at each peak angle moment for the spinal alignment using the reflective markers. SA refers to spinal alignment. The error bars were defined as means ± SD. Paired *t* tests were conducted for peak joint angles, revealing no statistically significant differences when participants wore the device.

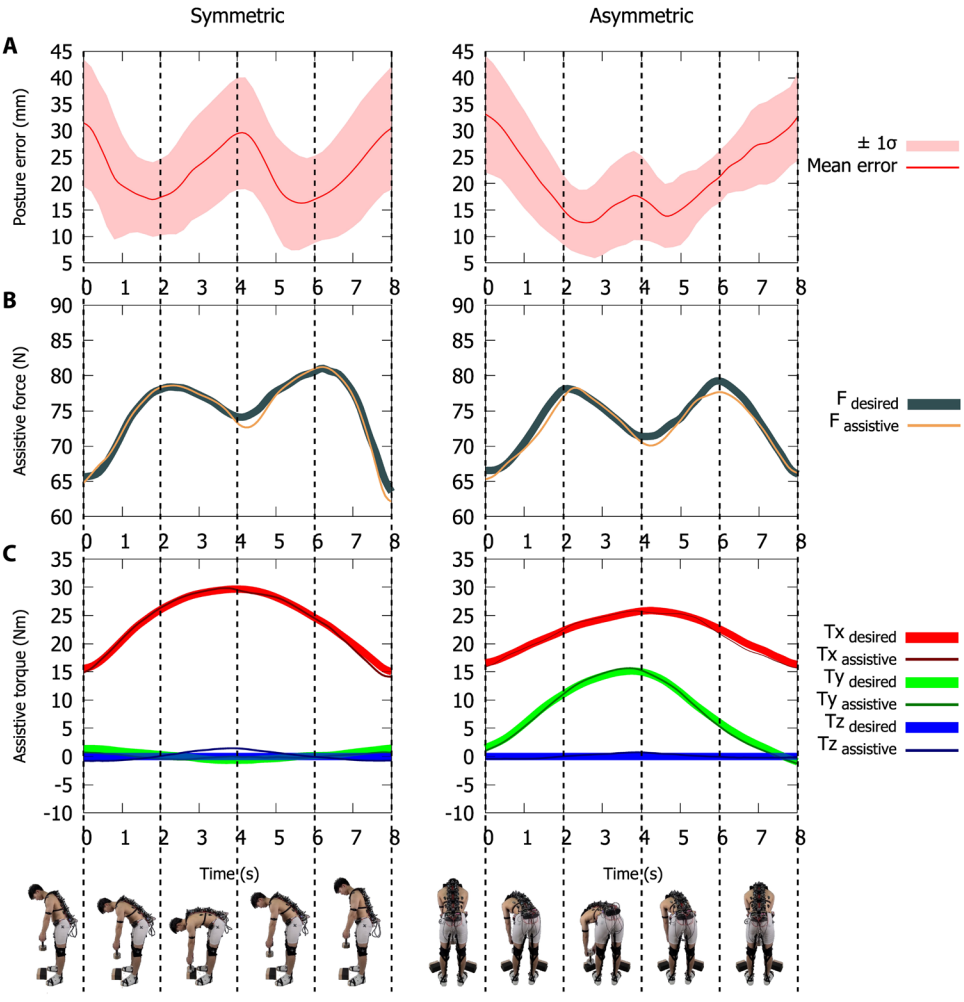

Fig. 5. Multi-DoF assistance. (**A**) Postural errors, (**B**) actual assistive force and desired assistive force, and (**C**) actual assistive torque and desired assistive torque during symmetric and asymmetric lifting tasks. Desired assistive force and torque were calculated to compensate for the effect of external weight.

by 20.60 and 52.87% in the symmetric and the asymmetric lifting tasks, respectively. For the semitendinosus (ST) and the gluteus maximus (GM), no statistically significant effects were observed in either lifting task. Through the muscle fatigue analysis, we confirmed that the BBEX reduced the effort of the back extensor muscles.

Body kinematics and joint reaction forces

We analyzed the effect of the BBEX on the kinematics of the wearer's body (Fig. 6C). In the symmetric lifting task, the BBEX did not alter the kinematics of the spine and the hip. There was no statistically significant effect on the peak joint angles of hip flexion and three major spinal motions: lumbar flexion, lateral bending, and axial rotation. However, in the asymmetric lifting task, the BBEX altered the kinematics of the spine. A two-way repeated measures ANOVA revealed a significance in the main effect of the BBEX on the peak joint angles of hip flexion and lumbar flexion. Subsequent paired *t* tests further confirmed that the BBEX exerted a statistically significant effect on the peak joint angles of hip flexion and lumbar flexion. With the BBEX, the peak lumbar flexion angle increased by 23.01% in the initial stage, 21.77% in the middle stage, and 18.23% in the final stage. On the other hand, the peak hip flexion angle decreased by 11.25% in the initial stage, 13.10% in the middle stage, and 13.16% in the final stage. Also, the peak axial rotation angle decreased by 13.58% in the initial stage, 29.17% in the middle stage, and 46.61% in the final stage.

We validated the effect of the BBEX on spinal loading by analyzing the joint compression forces of L1/L2, L2/L3, L3/L4, L4/L5, and L5/S1 (Fig. 6D). In both lifting tasks, the significant main effects of the BBEX were observed for the peak compression forces of all joints. Also, post hoc paired *t* tests revealed that the BBEX effectively decreased the joints' peak compression forces in all stages, and the results were statistically significant. With the BBEX, the peak compression force of the L5/S1 joint in the symmetric lifting task decreased by 15.6% in the initial stage, 15.4% in the middle stage, and 13.2% in the final stage. Similarly, the peak compression force of the L1/L2 joint decreased by 7.76% in the initial stage, 7.14% in the middle stage, and 5.24% in the final stage. In the asymmetric lifting task, the L5/S1 peak compression force decreased by 13.2% in the initial stage, 13.3% in the middle stage, and 15.2% in the final stage with the BBEX. In addition, the L1/L2 peak compression force decreased by 16.4% in the initial stage, 16.2% in the middle stage, and 17.4% in the final stage. The results for the other joints are summarized in table S1. Through the musculoskeletal analysis, we confirmed that the BBEX reduced the spinal loading of lower back joints.

DISCUSSION

The main contribution of this work is the design and validation of the BBEX, an active back-support device. We designed the BBEX inspired by the human spine and back extensor muscles to provide multidimensional force assistance and to ensure safety across the spine. We demonstrated that the BBEX achieved an effective alignment with the spine under various back movements, allowing the wearer's natural ROM. Also, we showed that the BBEX accurately estimated the wearer's back posture and provided multidimensional force assistance that changed according to the user's lifting posture. Last, we confirmed the potential of the BBEX to enhance overall spinal safety by alleviating key mechanical risk factors of lifting-induced lower back injuries through muscle fatigue and joint reaction analysis.

Through the repeated symmetric and asymmetric lifting tasks, we confirmed that the BBEX reduced muscle fatigue of the back extensor muscles, including the LE and UE, the main risk factor for spinal injuries. In particular, a more substantial reduction of muscle fatigue was observed in the asymmetric lifting task. Because the strength of available back extensor muscles decreased when performing asymmetric lifting, muscle fatigue appeared quickly. With

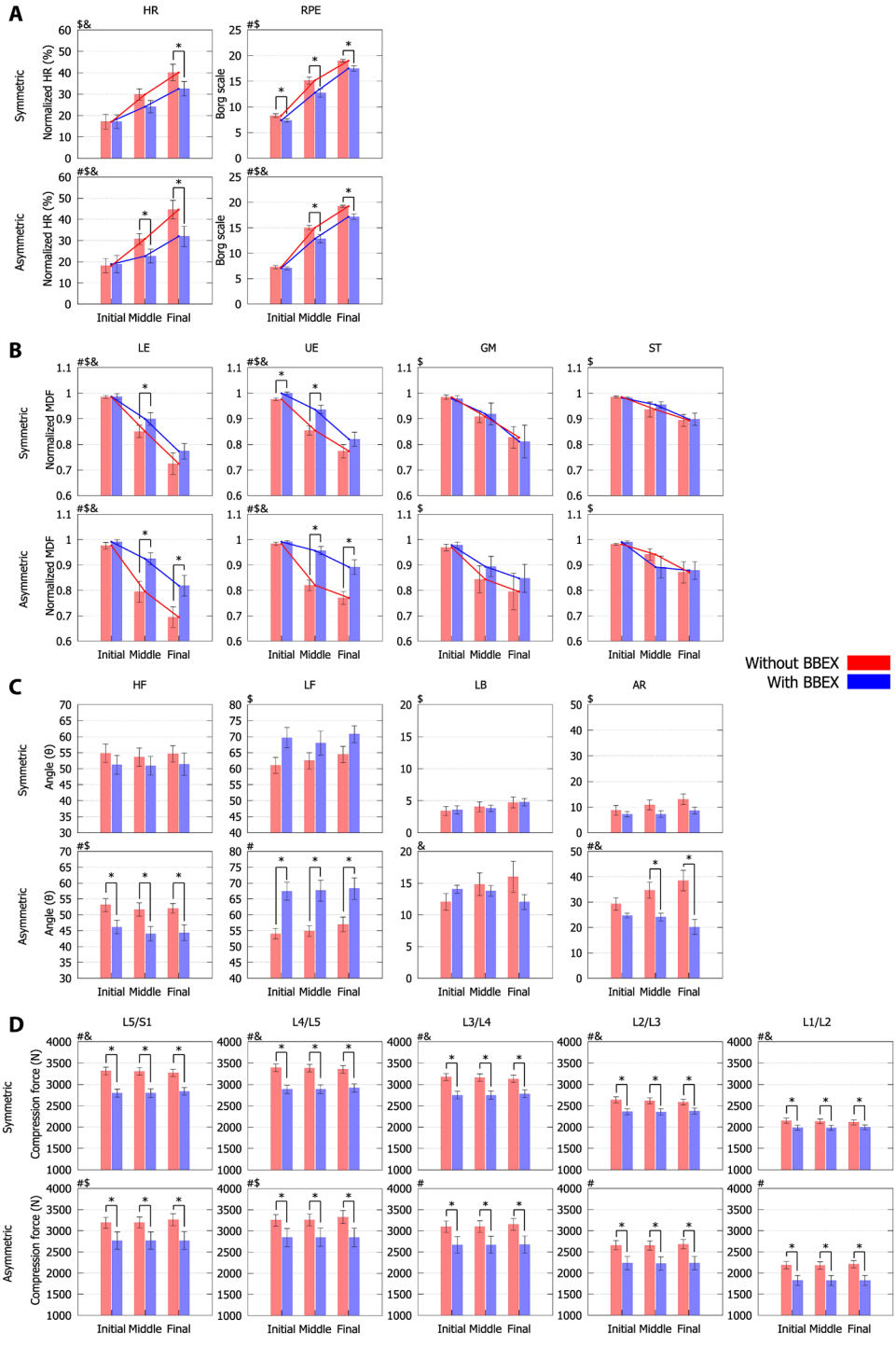

Fig. 6. Biomechanical and physiological results. (**A**) HR and RPE. Mean HR and RPE, averaged over all participants, were used. (**B**) Muscle fatigue for the LE, UE, ST, and GM. Mean MDF, averaged over all participants, was used. (**C**) Peak joint angles of hip flexion (HF), lumbar flexion (LF), lateral bending (LB), and axial rotation (AR). The mean peak joint angle, averaged over all participants, was used. (**D**) Compression forces on the L1/L2, L2/L3, L3/L4, L4/L5, and L5/S1 joints. Mean compression force, averaged over all participants, was used. Two-way repeated measures ANOVA tests were conducted considering device condition (without and with the BBEX), time condition (initial, middle, and final), and their interaction. Symbols #, $, and &, shown in the top-left corner of each graph, indicate the main effect of the device, the main effect of time, and the interaction between device and time, respectively. Subsequently, paired *t* tests were performed for variables with a significant main effect of the device or a significant interaction ($P < 0.05$). The symbol * denotes pairs where the BBEX device causes statistically significant differences. Error bars represent means ± SD.

the BBEX, this rapid drop in muscle fatigue was effectively suppressed by supplementing the decreased muscle strength. In addition, our findings indicate that the BBEX did not influence muscle fatigue in the hip extensors, including the GM and ST. Given that the bulk of the BBEX's weight was situated above the hip joint, it resulted in an increased external torque on the hip joint during lifting activities. This increase in torque necessitates compensation through the activation of the hip extensor muscles, specifically GM and ST. Consequently, under the BBEX condition, one might anticipate a relatively higher level of muscle fatigue in GM and ST. Nonetheless, our observations revealed no significant difference in muscle fatigue between these muscles. This result can be attributed to two possible explanations: The external torque generated by the BBEX's weight was sufficiently minimal to elicit an effect, or the BBEX effectively assisted not only spinal extension but also hip extension because of the lower anchoring mechanism, thereby effectively offsetting the external torque.

Musculoskeletal analysis revealed that the participants with the BBEX predominantly used the spinal mobility (trunk flexion) more than that of the hip joint. In both lifting tasks, the peak spinal flexion angle increased; on the other hand, the peak hip flexion angle decreased. These kinematic changes could be interpreted as participants adapting to the BBEX and adjusting their lifting techniques to take greater advantage of the back support of the BBEX. We also confirmed that the BBEX reduced the mechanical loadings across the lumbar joints. With the BBEX, the peak compression forces of the L1/L2, L2/L3, L4/L5, and L5/S1 joints decreased by an average of 11.03, 11.71, 13.65, 14.84, and 16.08% in the symmetric lifting task, respectively, and decreased by an average of 14.7, 14.06, 12.1, 10.93, and 11.7% in the asymmetric lifting task, respectively. Because the back extensor muscle force needed to counteract the moment of the upper body and external load increases the compression forces of the overall joints in the spine, it is conceivable that the assistive force generated by the BBEX, which acts as a

secondary back extensor muscle, could increase the compression forces on the spinal joints. However, the BBEX uses a larger moment arm than the back muscle about the spine, effectively providing the necessary restoration torque with less force. This can considerably reduce the required back muscle force, decreasing the compression forces of the overall spinal joints.

Although the BBEX performed well in all the experiments with human participants, there is still room for further improvement. Because inertial measurement unit (IMU) sensors were not attached to all modules of the BBEX for simplicity in the system, the orientation of each module was not accurately measured, and there was an unavoidable error in the wearer's posture. In particular, a relatively large error occurred in an upright posture because the BBEX had difficulties in estimating the S shape of a human spine. Even if the overall system becomes complex, integrating an IMU sensor into each module will improve the accuracy in estimating the wearer's posture. In addition, the versatility of the BBEX can be enhanced through an improved lower anchoring mechanism. In the current design, the bottom module of the BBEX is not firmly anchored in movements involving plantar flexion of the ankle, such as walking and running, because the strap from the bottom module to the overshoe is loosened during plantar flexion. A design approach unaffected by the movement of the ankle, for example, deploying straps on the sides of the lower extremities, could solve this anchoring issue and improve the device's versatility. Another improvement can be realized by optimizing the assistive force profile in the BBEX. The current force profile is determined by considering the wearer's kinematic posture. If the force profile is constructed to additionally consider the wearer's dynamics, then more improved assistance can be possible. Last, the joint reaction forces in the musculoskeletal analysis were calculated on the basis of the muscle forces estimated by the static optimization method in OpenSim, an open-source biomechanical modeling and simulation software system. The actual joint reaction forces might be more accurately quantified by using pressure sensors inserted between lumbar joints, as suggested in previous studies (*51*–*53*). In addition, considering that joint reaction forces are significantly influenced by the coactivation of agonist and antagonist muscles, which is a common phenomenon in maintaining stability, there is a possibility that our results might underestimate the true joint reaction forces (*54*, *55*). However, we maintain that the findings of this study hold substantial value given that a consistent methodology was applied uniformly across all the experimental procedures.

We developed the BBEX primarily to assist with the movement of the spine and validated it through the trunk-bending lifting tasks. Therefore, further studies with the BBEX will validate its efficacy for other lifting tasks with limited spinal movements, such as squatting and sitting to stand. In addition, to deepen our understanding of the asymmetric lifting, one of the characteristics of the BBEX, we will assess its effectiveness separately on the left and right muscles during repetitive lifting experiments on one side only. Subsequent studies will also explore the correlation between the mechanical properties of the BBEX and its assistance performance. For example, the effect of the robot's weight on the wearer can be verified through experiments wearing the device without providing assistance. We will also enhance the robot's control logic and demonstrate that assistance performance can be maintained consistently for lifting tasks at various speeds. Last, we will conduct long-term human trials. The data obtained from individual participants suggested that, for certain participants, their outcomes seemed to be influenced by their familiarity with the BBEX (Supplementary Discussion and fig. S11). Therefore, we plan to affirm how familiarity with the BBEX affects assistive performance. Also, a long-term analysis on how the BBEX affects the body will be included.

MATERIALS AND METHODS

Objective and design

The objective of this study was to design and evaluate the functionality and safety of the BBEX. The study involved 11 healthy male participants performing symmetric and asymmetric lifting tasks with and without the BBEX, creating two experimental conditions for comparison. The data were collected until the participants either stopped lifting or completed 30 lifts in each task. The data inclusion criteria were based on the successful completion of the tasks, excluding the data from participants who did not complete all the tasks. The primary metrics included the muscle fatigue, the HR, the RPE, the peak joint angles, and the peak joint reaction forces. The data were collected using surface electromyography (sEMG), a motion capture system, and HR monitors to assess the physiological and biomechanical impacts of the BBEX.

Instruments

HR and rating of perceived exertion

HRs were measured on the right upper arm using a HR monitor armband (Ticker Fit, Wahoo) at the end of every 8-s interval. RPEs were recorded by participants every three intervals with the Borg Scale table posted. When a participant reached a RPE of 20, we no longer needed to report the RPE because 20 is the maximum value.

Muscle electrical activity

sEMG signals were recorded by EMG electrodes (Trigno Wireless EMG System, Delsys Inc., Natick, MA, USA) at a sample rate of 2000 Hz. The attachment procedure of all EMG electrodes followed SENIAM (Surface Electromyography for the Non-Invasive Assessment of Muscles) guidelines. After cleaning with alcohol, eight surface electrodes were attached bilaterally over the following sites: LE (lumbar), UE (thoracic), GM, and ST. The positions of the EMG electrodes for lower and upper back extensors corresponded to levels of L3 and T10, respectively (*56*, *57*).

Body kinematics

A three-dimensional motion capture system with eight infrared cameras (Oqus 500, Qualisys, Sweden) equipped around the laboratory was used at a sampling rate of 100 Hz. The calibration system yielded a measurement error of less than 0.7 mm. Reflective markers (14-mm diameter) were attached to spinous process of the seventh cervical vertebra, bilateral acromion process of the scapular, posterior superior iliac spine of the pelvis, greater trochanter of the femur, medial and lateral femoral epicondyle, and medial and lateral malleolus of the ankle. In addition, 10 markers were attached to the suit (three for the top module, four for the middle modules, and three for the bottom module).

Participants

Eleven men who had no history of low back injury or musculoskeletal disorders volunteered to participate in the study. The means (SDs in parenthesis) of age, height, sitting height, and body mass of the participants were 25.73 years (0.96 years), 174.45 cm (3.06 cm), 89.91 cm (2.57 cm), and 76.36 kg (8.41 kg), respectively. Further

details on the participants are described in table S2. All participants received an information letter before the experiments and signed an informed consent form.

Experimental procedure

All participants performed two types of tasks, a symmetric lifting task and an asymmetric lifting task, and conducted each task twice, with and without the BBEX. Thus, a total of four experiments were conducted for each participant. Each experiment was performed at intervals of 1 week to exclude the effects of the previous experiment. All experimental procedures performed in the study were approved by the Institutional Review Board of Seoul National University (Institutional Review Board no. 1912/001-003), and all participants were familiarized with the experimental procedures and the BBEX before the experiments. In the preparation process, EMG electrodes and reflective markers were attached to the participants, and a HR monitor armband was placed on their right upper arm. For the experiments with the device, the BBEX was fitted and adjusted to the individual participants. Subsequently, reflective markers were attached to the suit as well. After the preparation, the participants took a 5-min break (*58*) to relieve any fatigue that might occur during the preparation process. The participants lowered and lifted a weight of 5.5 kg 30 times with an interval of 8 s for each experiment. In the symmetric lifting task, the participants performed the cyclic lifting task in the sagittal plane to touch a pad in front of the foot. In the asymmetric lifting task, the participants performed the lifting by rotating the trunk alternately left and right side to touch a pad, which was located ±45° to the sagittal plane. We provided auditory feedback using a metronome to control lifting speed, and the participants were asked to handle the weight at a constant speed as smoothly as possible. The weight and the lifting interval were chosen to follow the limits suggested by the National Institute for Occupational Safety and Health Guidelines while guaranteeing 30 continuous lifts (*59*). Because the lower back extensor muscles become silent in the upright posture, we limited the maximum range of extension during the upward-lifting phase to induce sustained muscle contraction. To prevent the involvement of the lower extremities, participants were asked not to bend their knees and were instructed to keep the weight within the marked area on the floor. The ground level of the floor on which the individual participants put their feet was adjusted using a platform in consideration of the participants' ROM (see movie S7 for the experiment description).

Data analysis

Data from one participant in the symmetric lifting task and two participants in the asymmetric lifting task were discarded because of IMU data storage failure. Therefore, data analysis was performed with the results of 10 participants for the symmetric lifting task and nine participants for the asymmetric lifting task.

HR and rating of perceived exertion

HR was normalized using resting and maximum HR. The resting HR was measured at rest before the experiment. The maximum HR was applied differently according to the age of the participants (*60*). Normalized HR was calculated by dividing the difference between the current and the resting HR by the difference between the maximum and the resting HR.

Muscle fatigue

Muscle fatigue was analyzed using sEMG signals. The raw sEMG signals were filtered using a second-order Butterworth band-pass filter with a frequency range of 5 to 500 Hz. Because the sEMG signals were obtained during isotonic muscle contractions, the continuous wavelet transform was used to obtain the time-frequency response of each target muscle. The Morlet wavelet was selected as the mother wavelet, and the wavelet scale length was selected to be 128 to obtain the scalogram. The MDF was used as an index for muscle fatigue assessment considering that muscle fatigue results in a downward shift of the frequency spectrum of sEMG signals (*61*). In the maximal flexion posture corresponding to the lowest point of the marker attached to C7, the muscle activity patterns varied among the participants depending on their flexibility properties. Therefore, we chose the time event of MDF analysis on the basis of the maximum extension posture when the marker attached to C7 reaches the highest point. This maximum extension posture could be seen as a transition point in the type of muscle contraction because the spinal extensor muscles switch from concentric to eccentric contractions. To reflect the characteristics of this dynamic contraction, 2 s before and after the maximum extension posture was set as the analysis window. Because the initial MDF values were different for each participant and each muscle, all MDF values were normalized to the initial MDF values. In addition, because the surface electrodes were attached bilaterally on the target muscles, the averaged MDF value of both sides was used as a representative value. All data for the MDF analysis were processed with MATLAB R2020b (MathWorks).

Body kinematics and mechanical joint work

A musculoskeletal analysis using OpenSim was conducted to evaluate the effect of the BBEX on body kinematics and joint compressive forces. We used a revised full-body lumbar spine (FBLS) model, which corrects the DoFs of the original FBLS model, as Beaucage-Gauvreau *et al.* suggested (*34*, *62*, *63*). The analyses were conducted in the order of scaling, inverse kinematics, inverse dynamics, static optimization, and joint analysis. The base model was transformed into the individualized model for each participant using the scaling tool. The scaling tool was conducted on the basis of 11 markers that were attached to participants in the experiments without the BBEX. The mass of the OpenSim model was also modulated to reflect the inertia of the device and the weight used in the experiment: A mass of 2.75 kg was uniformly added to each hand, whereas an additional 4 kg was placed on the pelvis and 1.75 kg on the torso. Body kinematics of the participants were first calculated with an inverse kinematics tool using real-time marker data and then low-pass–filtered with a cutoff frequency of 2 Hz. In this process, elbow marker data were added using the estimated humerus length and the shoulder markers' data (*64*). To analyze the kinematic change of hip and spinal joints during lifting experiments, peak joint angles of hip flexion/extension, lumbar flexion, lateral bending, and axial rotation were calculated in each cycle and then averaged over five cycles for each stage. Also, we derived the external loads on participants to compute joint compressive forces. In the experiments with human participants, the external loads were assistive forces from the BBEX and ground reaction forces (GRFs). We modeled the assistive forces on the basis of the BBEX design and calculated the magnitude and position of GRF using residual forces/moments, as Dijkstra and Gutierrez-Farewik (*65*) have proposed (details on modeling of external loads for musculoskeletal analysis can be found in Supplementary Methods). Then, we assessed the efficacy of the BBEX on the compressive forces of the lumbar joints using the joint reaction analysis tool of OpenSim. Peak joint compressive forces of the L1/

L2, L2/L3, L3/L4, L4/L5, and L5/S1 joints during each lifting cycle were averaged over five cycles for each stage after low-pass filtering with a cutoff frequency of 0.5 Hz.

Statistics

Statistical analysis was conducted using R (RStudio Inc., Boston, MA, USA) to examine whether the effects of the BBEX were statistically significant. Independent variables of this analysis were the existence and nonexistence of the BBEX (referred to as with the BBEX or without the BBEX) and experiment time (referred to as initial, middle, and final stages). Dependent variables were the MDF of the EMG signal, peak body kinematics, peak joint reaction forces, normalized HR, and RPE. In each experiment, the dependent variables were divided into initial, middle, and final stages according to time. EMG signal, peak body kinematics, peak joint reactions, and normalized HR that were measured every lifting cycle were averaged over the initial five cycles, middle five cycles, and last five cycles and were labeled as "initial," "middle," and "final." Similarly, RPE data were averaged over the initial, middle, and last two cycles and equivalently labeled. To analyze the interaction between two independent variables on dependent variables, two-way repeated measures ANOVA tests were conducted. Sequentially, post hoc paired *t* tests were followed and analyzed with false detection rate when significant main effects of the device or interaction were identified. The normality of the dependent variables was tested using Shapiro-Wilk's test and visual inspection through QQ-plots. Mauchly's test of sphericity was conducted for all results, and a Greenhouse-Geisser correction was used when the sphericity assumption was violated. The critical level of significance was set to alpha = 0.05.

Supplementary Materials

The PDF file includes:

Methods
Discussion
Figs. S1 to S11
Tables S1 and S2

Other Supplementary Material for this manuscript includes the following:

Movies S1 to S7
MDAR Reproducibility Checklist

REFERENCES AND NOTES

1. A. Wu, L. March, X. Zheng, J. Huang, X. Wang, J. Zhao, F. M. Blyth, E. Smith, R. Buchbinder, D. Hoy, Global low back pain prevalence and years lived with disability from 1990 to 2017: Estimates from the Global Burden of Disease Study 2017. *Ann. Transl. Med.* **8**, 299–313 (2020).
2. R. Buchbinder, M. van Tulder, B. Öberg, L. M. Costa, A. Woolf, M. Schoene, P. Croft, R. Buchbinder, J. Hartvigsen, D. Cherkin, N. E. Foster, C. G. Maher, M. Underwood, M. van Tulder, J. R. Anema, R. Chou, S. P. Cohen, L. M. Costa, P. Croft, M. Ferreira, P. H. Ferreira, J. M. Fritz, S. Genevay, D. P. Gross, M. J. Hancock, D. Hoy, J. Karppinen, B. W. Koes, A. Kongsted, Q. Louw, B. Öberg, W. C. Peul, G. Pransky, M. Schoene, J. Sieper, R. J. Smeets, J. A. Turner, A. Woolf, Low back pain: A call for action. *Lancet* **391**, 2384–2388 (2018).
3. J. Hartvigsen, M. J. Hancock, A. Kongsted, Q. Louw, M. L. Ferreira, S. Genevay, D. Hoy, J. Karppinen, G. Pransky, J. Sieper, R. J. Smeets, M. Underwood, Lancet Low Back Pain Series Working Group, What low back pain is and why we need to pay attention. *Lancet* **391**, 2356–2367 (2018).
4. R. Z. Goetzel, K. Hawkins, R. J. Ozminkowski, S. Wang, The health and productivity cost burden of the "top 10" physical and mental health conditions affecting six large US employers in 1999. *J. Occup. Environ. Med.* **45**, 5–14 (2003).
5. J. Hamill, K. M. Knutzen, *Biomechanical Basis of Human Movement* (Lippincott Williams & Wilkins, 2006).
6. M. R. Bracko, Can we prevent back injuries? *ACSMs Health Fit. J.* **8**, 5–11 (2004).
7. S. M. McGill, The biomechanics of low back injury: Implications on current practice in industry and the clinic. *J. Biomech.* **30**, 465–475 (1997).
8. T. J. Noonan, W. E. Garrett Jr., Muscle strain injury: Diagnosis and treatment. *J. Am. Acad. Orthop. Surg.* **7**, 262–269 (1999).
9. L. C. Brereton, S. M. McGill, Effects of physical fatigue and cognitive challenges on the potential for low back injury. *Hum. Mov. Sci.* **18**, 839–857 (1999).
10. G. Shin, C. D'Souza, Y. H. Liu, Creep and fatigue development in the low back in static flexion. *Spine* **34**, 1873–1878 (2009).
11. P. Dolan, M. A. Adams, Repetitive lifting tasks fatigue the back muscles and increase the bending moment acting on the lumbar spine. *J. Biomech.* **31**, 713–721 (1998).
12. S. H. Kim, M. K. Chung, Rapid communication effects of posture, weight and frequency on trunk muscular activity and fatigue during repetitive lifting tasks. *Ergonomics* **38**, 853–863 (1995).
13. M. A. Adams, N. Bogduk, K. Burton, P. Dolan, *The Biomechanics of Back Pain* (Elsevier Health Sciences, 2012).
14. M. F. Antwi-Afari, H. Li, D. J. Edwards, E. A. Pärn, J. Seo, A. Y. L. Wong, Biomechanical analysis of risk factors for work-related musculoskeletal disorders during repetitive lifting task in construction workers. *Autom. Constr.* **83**, 41–47 (2017).
15. P. J. Sparto, M. Parnianpour, T. E. Reinsel, S. Simon, The effect of fatigue on multijoint kinematics, coordination, and postural stability during a repetitive lifting test. *J. Orthop. Sports Phys. Ther.* **25**, 3–12 (1997).
16. T. R. Waters, V. Putz-Anderson, A. Garg, L. J. Fine, Revised NIOSH equation for the design and evaluation of manual lifting tasks. *Ergonomics* **36**, 749–776 (1993).
17. A. L. Barrett, Evaluation of four weight transfer devices for reducing loads on lower back during agricultural stoop labor, paper presented at the Annual International Meeting of the American Society of Agricultural Engineers, St. Joseph, MI, July to August 2001 (ASAE, 2001), paper no. 1-8056.
18. M. Wehner, D. Rempel, H. Kazerooni, "Lower extremity exoskeleton reduces back forces in lifting" in *ASME 2009 Dynamic Systems and Control Conference* (American Society of Mechanical Engineers, 2009), pp. 49–56.
19. B. L. Ulrey, F. A. Fathallah, Effect of a personal weight transfer device on muscle activities and joint flexions in the stooped posture. *J. Electromyogr. Kinesiol.* **23**, 195–205 (2013).
20. B. L. Ulrey, F. A. Fathallah, Subject-specific, whole-body models of the stooped posture with a personal weight transfer device. *J. Electromyogr. Kinesiol.* **23**, 206–215 (2013).
21. H. Yu, I. S. Choi, K. L. Han, J. Y. Choi, G. Chung, J. Suh, Development of a stand-alone powered exoskeleton robot suit in steel manufacturing. *ISIJ Int.* **55**, 2609–2617 (2015).
22. H. Zhang, A. Kadrolkar, F. C. Sup, Design and preliminary evaluation of a passive spine exoskeleton. *J. Med. Devices.* **10**, 011002 (2016).
23. S. Toxiri, A. Calanca, J. Ortiz, P. Fiorini, D. G. Caldwell, A parallel-elastic actuator for a torque-controlled back-support exoskeleton. *IEEE Robot. Autom. Lett.* **3**, 492–499 (2017).
24. S. Toxiri, A. S. Koopman, M. Lazzaroni, J. Ortiz, V. Power, M. P. De Looze, D. G. Caldwell, Rationale, implementation and evaluation of assistive strategies for an active back-support exoskeleton. *Front. Robot. AI* **5**, 53 (2018).
25. X. Yong, Z. Yan, C. Wang, C. Wang, N. Li, X. Wu, Ergonomic mechanical design and assessment of a waist assist exoskeleton for reducing lumbar loads during lifting task. *Micromachines* **10**, 463 (2019).
26. H. Kazerooni, W. Tung, M. Pillai, "Evaluation of trunk-supporting exoskeleton" in *Proceedings of the Human Factors and Ergonomics Society Annual Meeting* (SAGE Publications, 2019), pp. 1080–1083.
27. T. Bosch, J. van Eck, K. Knitel, M. de Looze, The effects of a passive exoskeleton on muscle activity, discomfort and endurance time in forward bending work. *Appl. Ergon.* **54**, 212–217 (2016).
28. H. K. Ko, S. W. Lee, D. H. Koo, I. Lee, D. J. Hyun, Waist-assistive exoskeleton powered by a singular actuation mechanism for prevention of back-injury. *Rob. Auton. Syst.* **107**, 1–9 (2018).
29. Z. Yao, C. Linnenberg, R. Weidner, J. Wulfsberg, "Development of a soft power suit for lower back assistance" in *Proceedings of the 2019 IEEE International Conference on Robotics and Automation* (IEEE, 2019), pp. 5103–5109.
30. ATOUN, INC., Atoun Model Y (2020); http://atoun.co.jp/products/atoun-model-y [accessed 26 March 2022].
31. Panasonic, Activelink, AWN-03 (2020); https://news.panasonic.com/global/stories/2016/44969.html [accessed 26 March 2022].
32. H. S. Seong, D. H. Kim, I. Gaponov, J. H. Ry, "Development of a twisted string actuator-based exoskeleton for hip joint assistance in lifting tasks" in *Proceedings of the 2020 IEEE International Conference on Robotics and Automation* (IEEE, 2020), pp. 761–767.
33. K. Naruse, S. Kawai, H. Yokoi, Y. Kakazu, "Development of wearable exoskeleton power assist system for lower back support" in *Proceedings 2003 IEEE/RSJ International Conference on Intelligent Robots and Systems* (IEEE, 2003), pp. 3630–3635.
34. S.-S. Yun, K. Kim, J. Ahn, K.-J. Cho, Body-powered variable impedance: An approach to augmenting humans with a passive device by reshaping lifting posture. *Sci. Robot.* **6**, eabe1243 (2021).
35. R. Bini, D. Wundersitz, M. Kingsley, Biomechanical and physiological responses to electrically assisted cycling during simulated mail delivery. *Appl. Ergon.* **75**, 243–249 (2019).

36. T. Zhang, H. Huang, A lower-back robotic exoskeleton: Industrial handling augmentation used to provide spinal support. *IEEE Robot. Automat. Mag.* **25**, 95–106 (2018).
37. M. B. Näf, A. S. Koopman, S. Baltrusch, C. Rodriguez-Guerrero, B. Vanderborght, D. Lefeber, Passive back support exoskeleton improves range of motion using flexible beams. *Front. Robot. AI* **5**, 72 (2018).
38. S. J. Baltrusch, J. H. Van Dieën, A. S. Koopman, M. B. Näf, C. Rodriguez-Guerrero, J. Babič, H. Houdijk, SPEXOR passive spinal exoskeleton decreases metabolic cost during symmetric repetitive lifting. *Eur. J. Appl. Physiol.* **120**, 401–412 (2020).
39. M. M. Alemi, J. Geissinger, A. A. Simon, S. E. Chang, A. T. Asbeck, A passive exoskeleton reduces peak and mean EMG during symmetric and asymmetric lifting. *J. Electromyogr. Kinesiol.* **47**, 25–34 (2019).
40. A. A. Simon, M. M. Alemi, A. T. Asbeck, Kinematic effects of a passive lift assistive exoskeleton. *J. Biomech.* **120**, 110317 (2021).
41. T. Schmalz, A. Colienne, E. Bywater, L. Fritzsche, C. Gärtner, M. Bellmann, M. Ernst, A passive back-support exoskeleton for manual materials handling: Reduction of low back loading and metabolic effort during repetitive lifting. *IISE Trans. Occup. Ergon. Hum. Factors* **10**, 7–20 (2021).
42. X. Yang, T. H. Huang, H. Hu, S. Yu, S. Zhang, X. Zhou, A. Carriero, G. Yue, H. Su, Spine-inspired continuum soft exoskeleton for stoop lifting assistance. *IEEE Rob. Autom. Lett.* **4**, 4547–4554 (2019).
43. J. M. Li, D. D. Molinaro, A. S. King, A. Mazumdar, A. J. Young, Design and validation of a cable-driven asymmetric back exosuit. *IEEE Trans. Robot.* **38**, 1489–1502 (2021).
44. S. Standring, H. Ellis, J. Healy, D. Johnson, A. Williams, P. Collins, C. Wigley, Gray's anatomy: The anatomical basis of clinical practice. *AJNR Am. J. Neuroradiol.* **26**, 2703 (2005).
45. F. Heuer, H. Schmidt, L. Claes, H. J. Wilke, Stepwise reduction of functional spinal structures increase vertebral translation and intradiscal pressure. *J. Biomech.* **40**, 795–803 (2007).
46. N. V. Jaumard, W. C. Welch, B. A. Winkelstein, Spinal facet joint biomechanics and mechanotransduction in normal, injury and degenerative conditions. *J. Biomech. Eng.* **133**, 071010 (2011).
47. J. I. Kim, J. Choi, J. Kim, Y.-L. Park, A Twisted Elastic Rotary-Rail Actuator (TERRA) using a double-stranded helix structure. *IEEE Robot. Autom. Lett.* **6**, 7381–7388 (2021).
48. D. E. Rassier, B. R. MacIntosh, W. Herzog, Length dependence of active force production in skeletal muscle. *J. Appl. Physiol.* **86**, 1445–1457 (1999).
49. A. T. Asbeck, S. M. De Rossi, K. G. Holt, C. J. Walsh, A biologically inspired soft exosuit for walking assistance. *Int. J. Rob. Res.* **34**, 744–762 (2015).
50. A. S. Iberall, "The use of lines of nonextension to improve mobility in full-pressure suits," AMRL-TR-64-118 (RAND DEVELOPMENT CORP, 1964).
51. A. Schultz, G. Andersson, R. Ortengren, K. Haderspeck, A. Nachemson, Loads on the lumbar spine. Validation of a biomechanical analysis by measurements of intradiscal pressures and myoelectric signals. *J. Bone Joint Surg.* **64**, 713–720 (1982).
52. H. J. Wilke, P. Neef, B. Hinz, H. Seidel, L. Claes, Intradiscal pressure together with anthropometric data – A data set for the validation of models. *Clin. Biomech.* **16**, S111–S126 (2001).
53. A. Nachemson, In vivo measurements of intradiscal pressure. *J. Bone. Joint. Surg.* **146**, 1877–1892 (1990).
54. W. S. Marras, C. M. Sommerich, A three-dimensional motion model of loads on the lumbar spine: I. Model Structure. *Hum. Factors* **33**, 123–137 (1991).
55. K. P. Granata, W. S. Marras, The influence of trunk muscle coactivity on dynamic spinal loads. *Spine* **20**, 913–919 (1995).
56. R. B. Graham, M. J. Agnew, J. M. Stevenson, Effectiveness of an on-body lifting aid at reducing low back physical demands during an automotive assembly task: Assessment of EMG response and user acceptability. *Appl. Ergon.* **40**, 936–942 (2009).
57. P. Dolan, I. Kingma, M. P. De Looze, J. H. Van Dieen, H. M. Toussaint, C. T. M. Baten, M. A. Adams, An EMG technique for measuring spinal loading during asymmetric lifting. *Clin. Biomech.* **16**, S17–S24 (2001).
58. H. J. Shin, J. Y. Kim, Measurement of trunk muscle fatigue during dynamic lifting and lowering as recovery time changes. *Int. J. Ind. Ergon.* **37**, 545–551 (2007).
59. G. S. Nelson, H. Wickes, J. T. English, *Manual Lifting: The NIOSH Work Practices Guide for Manual Lifting Determining Acceptable Weights of Lift* (US Department of Health and Human Services, 1981).
60. S. M. Fox III, J. P. Naughton, W. L. Haskell, Physical activity and the prevention of coronary heart disease. *Ann. Clin. Res.* **3**, 404–432 (1971).
61. P. Bonato, G. R. Ebenbichler, S. H. Roy, S. Lehr, M. Posch, J. Kollmitzer, U. Della Croce, Muscle fatigue and fatigue-related biomechanical changes during a cyclic lifting task. *Spine* **28**, 1810–1820 (2003).
62. M. E. Raabe, A. M. W. Chaudhari, An investigation of jogging biomechanics using the full-body lumbar spine model: Model development and validation. *J. Biomech.* **49**, 1238–1243 (2016).
63. E. Beaucage-Gauvreau, W. S. P. Robertson, S. C. E. Brandon, R. Fraser, B. J. C. Freeman, R. B. Graham, D. Thewlis, C. F. Jones, Validation of an OpenSim full-body model with detailed lumbar spine for estimating lower lumbar spine loads during symmetric and asymmetric lifting tasks. *Comput. Methods Biomech. Biomed. Engin.* **22**, 451–464 (2019).
64. J. H. Lee, Y. S. Kim, U. Y. Lee, D. K. Park, Y. K. Jeong, N. S. Lee, S. Y. Han, S. H. Han, Stature estimation from partial measurements and maximum length of lower limb bones in Koreans. *Aust. J. Forensic Sci.* **46**, 330–338 (2014).
65. E. J. Dijkstra, E. M. Gutierrez-Farewik, Computation of ground reaction force using zero moment point. *J. Biomech.* **48**, 3776–3781 (2015).

Acknowledgments

Funding: This work was supported, in part, by the National Research Foundation of Korea (grant nos. RS-2023-00208052 and NRF-2019R1F1A1061871) funded by the Korean government (MSIT) and, in part, by the Technology Innovation Program (grant no. 20008912) funded by the Korean government (MOTIE). **Author contributions:** Conceptualization of SES mechanism: J.I.K. Design of the BBEX: J.I.K. Design of the anchoring mechanism: J.C. Design of the electrical parts: J.K. Fabrication of the BBEX: J.I.K., J.C., and J.K. Design of the functional testing experiment: J.I.K., J.C., and J.K. Analysis of the spinal alignment: J.I.K. Analysis of the ROM: J.C. Design of the human-subject experiment: J.I.K., J.C., J.K., and J.S. Analysis of the BBEX's kinematic model: J.I.K. Analysis of the posture estimation: J.I.K. Analysis of the multi-DoF assistance: J.I.K. Analysis of the HR and RPE: J.K. Analysis of the muscle fatigue: J.I.K. Analysis of the body kinematics and joint reaction forces: J.C. and J.K. Theoretical analysis of the multidimensional assistance: J.C. Theoretical analysis of the kinetically aligned force assistance: J.C. Statistics: J.C. Control of the BBEX: J.I.K. Modeling of the 4R-TERRA: J.C. and J.I.K. Supervision: J.P. and Y.-L.P. Writing—original draft: J.I.K., J.C., J.K., J.S., J.P., and Y.-L.P. **Competing interests:** A US patent application (serial no. 18/558,069) and a Korea (ROK) patent application (serial no. 1020220083838) related to part of this work were filed on 30 October 2023 and 7 July 2022, respectively. Y.-L.P., J.I.K., J.C., and J.K. are listed as coinventors. The other authors declare that they have no competing interests. **Data and materials availability:** All data needed to support the conclusions of this manuscript are included in the main text or Supplementary Materials. Data and code can also be found on Dryad: https://doi.org/10.5061/dryad.fbg79cp45.

Submitted 7 September 2023
Accepted 25 June 2024
Published 24 July 2024
10.1126/scirobotics.adk6717

Science Robotics

Bilateral Back Extensor Exosuit for multidimensional assistance and prevention of spinal injuries

Jae In Kim, Jaeyoun Choi, Junhyung Kim, Junkyung Song, Jaebum Park, and Yong-Lae Park

Sci. Robot. **9** (92), eadk6717. DOI: 10.1126/scirobotics.adk6717

Editor's summary
Repetitive tasks involving lifting of objects such as in industrial settings can cause injuries to the spine and back muscles. Although wearable exoskeleton suits can be used in these settings to alleviate risks to injury, they may not provide multidimensional movement during asymmetric lifting. Kim *et al.* have developed an active Bilateral Back Extensor Exosuit capable of multidimensional force assistance during lifting tasks. The wearable device offers multiple degrees of freedom in range of motion and was shown to provide back muscle force assistance and to decrease compression on the spines of human participants during asymmetric and symmetric lifting tasks. —Amos Matsiko

Science Robotics (ISSN 2470-9476) is published by the American Association for the Advancement of Science. 1200 New York Avenue NW, Washington, DC 20005. The title *Science Robotics* is a registered trademark of AAAS.